



Characterization of mechanical relaxation in a Cu–Zr–Al metallic glass



Chaoren Liu^a, Eloi Pineda^{b,*}, Daniel Crespo^a

^a Dept. Física Aplicada, EPSC, Universitat Politècnica Catalunya – BarcelonaTech, Esteve Terradas 5, 08860 Castelldefels, Spain

^b Dept. Física i Enginyeria Nuclear, ESAB, Universitat Politècnica Catalunya – BarcelonaTech, Esteve Terradas 8, 08860 Castelldefels, Spain

ARTICLE INFO

Article history:

Available online 1 November 2014

Keywords:

Amorphous alloys
Aging
Johari–Goldstein relaxation
Mechanical spectroscopy
Glass dynamics

ABSTRACT

The temperature dependence of the relaxation times of Cu₄₆Zr₄₆Al₈ glass was measured by means of mechanical spectroscopy and static stress–relaxation measurements. The weak intensity of secondary relaxation in this alloy allows us to correlate the characteristic times of dynamic and static measurements of primary relaxation. The glassy dynamics of an isoconfigurational state are found to follow an Adam–Gibbs–Vogel expression with the glassy state defined by a fictive temperature. The combination of both measurements proves that, in the frequency domain, the relaxation response can be well described by a single relaxation function above and below the glass transition. The change in relaxation times as function of the fictive temperature and the corresponding effects on the mechanical behavior are estimated and discussed.

© 2014 Elsevier B.V. All rights reserved.

1. Introduction

The structural dynamics of glasses is perceptible by probing different physical properties. In the liquid state, the characteristic times corresponding to different transport properties like viscosity, conductivity or diffusivity may show specific behaviors, but they all become strongly coupled near the glass transition. In the case of structural glasses, the relaxation of the structure is commonly explored applying static or oscillating electrical, mechanical or thermal stresses [1]. In many systems, the temperature dependence of the relaxation times above the glass transition temperature, T_g , can be described by a Vogel–Fulcher–Tammann (VFT) equation [2–5]

$$\tau_{\text{VFT}}(T) = \tau_0 \exp\left(\frac{B}{T - T_0}\right) \quad (1)$$

where B and T_0 are empirical parameters characterizing the time dependence of a particular substance. The VFT function is usually not able to describe the liquid phase dynamics in the whole temperature range; the validity of Eq. (1) is in general restricted to a range of temperatures just above T_g .

The diverging slowing down of the liquid dynamics when $T \rightarrow T_0$ is stopped when the system becomes arrested in the non-equilibrium glassy state. At temperatures below glass transition,

an equation proposed to describe the dynamics of the glassy state is [6]

$$\tau_{\text{AGV}}(T) = \tau_0 \exp\left[\frac{B}{T(1 - T_0/T_f)}\right] \quad (2)$$

where T_f is the fictive temperature defined as the point where the glass behavior converges with the liquid. In this work we will call Eq. (2) as the Adam–Gibbs–Vogel (AGV) function [7]. Within the approach to glassy dynamics given by the AGV-function, T_f is the parameter defining the particular isoconfigurational glassy state achieved during the cooling process. Eq. (2) is equivalent to consider an Arrhenius behavior of the relaxation time with activation energy $E_{\text{act}} = RB/(1 - T_0/T_f)$.

The non-equilibrium glassy phase is susceptible to change towards more stable configurations, this process is termed physical aging or structural relaxation and drives the glass to configurations with slower dynamics. Because of aging the relaxation times may change orders of magnitude [8,9], going from $\sim 10^2$ seconds to hundreds of hours or years depending on the temperature and the particular glassy state. The intrinsic relationship between the aging time and the relaxation time makes the time-evolving dynamics of glasses below T_g a complex non-linear problem [10]. Secondary or β -relaxations, faster than the main α -relaxation, are also a characteristic phenomenon of glassy systems. Usually, β -relaxations show an Arrhenius behavior below some departure point where they decouple from the main relaxation [11]. Although the presence of a secondary relaxation seems a universal feature of the glass transition, the microscopic origin, decoupling

* Corresponding author. Tel.: +34 935 521 141.

E-mail addresses: chaorenliu@gmail.com (C. Liu), eloi.pineda@upc.edu (E. Pineda), daniel.crespo@upc.edu (D. Crespo).

temperature, intensity and activation energy are unclear in many glassy substances.

In metallic glasses, the α -relaxation times are typically obtained from viscosity, calorimetric or mechanical spectroscopy measurements. Above T_g , the relaxation times are usually well described by a VFT behavior [12–16]. Below T_g , physical aging may change the system state by annihilation of excess free volume [17] or other structural changes [18], while the dynamics of isoconfigurational glassy states follows Arrhenius behaviors [19,20]. Mechanical spectroscopy revealed the presence of β -relaxations in metallic glasses [21]. Some systems show a prominent β -relaxation peak [22,23], while other systems does not show an evident secondary relaxation but just a low-temperature excess wing of the main relaxation peak [24–27]. The presence of pronounced β -relaxations in metallic glasses has recently been associated to similar negative heats of mixing between the constituting elements of the alloy [28].

Interestingly, there is a link between the activation energy of relaxations below T_g and the initiation of mechanical flow events [29–31] and, moreover, secondary relaxations are also considered the origin of physical aging or structural relaxation below T_g [32,33]. Physical aging and the corresponding change of fictive temperature may drive metallic glasses from ductile to brittle fracture behavior [34,35] or change chemical properties like the corrosion resistance [36]. The understanding of the relaxation spectrum of metallic glasses is then a key knowledge to control their properties and it has deep technological implications.

In this work we study the relaxation dynamics of $\text{Cu}_{46}\text{Zr}_{46}\text{Al}_8$ combining mechanical spectroscopy and static stress-relaxation tensile measurements. The response in mechanical spectroscopy is determined by a complex Young's modulus $E^*(\omega, T) = E'(\omega, T) + iE''(\omega, T)$. Micro-alloying of Al in the Cu–Zr–Al system suppresses the low temperature shoulder of the α -relaxation peak and the relaxation below T_g is only perceived as an excess wing of the $E''(\omega, T)$ [28]. We will show that the full shape of the experimental $E''(T)$ can be understood considering a single Cole–Cole (CC) relaxation function

$$E^*(\omega, T) = E_0(T) \left[1 - \frac{1}{1 + (i\omega\tau(T))^\alpha} \right] \quad (3)$$

with $\tau(T) = \tau_{\text{VFT}}(T)$ and $\tau(T) = \tau_{\text{AGV}}(T)$ above and below T_g respectively. The α parameter in Eq. (3) characterizes the broadening of the relaxation peak. The validity of this model will be confirmed by means of static measurements of stress-relaxation, which give us direct access to the time domain response. We will also compare the relaxation response between as-quenched and relaxed glasses. We will show that the low-temperature, slow relaxations of $\text{Cu}_{46}\text{Zr}_{46}\text{Al}_8$ are described by the proposed VFT-AGV scheme if the glassy state do not suffer significant structural changes during the measurement. Finally, we will discuss the implications of the relaxation scheme proposed here on the mechanical properties of metallic glasses.

2. Materials and methods

Master alloy with a nominal composition of $\text{Cu}_{46}\text{Zr}_{46}\text{Al}_8$ was prepared by arc melting a mixture of constituent elements with a purity of above 99.9% under a Ti-gettered argon atmosphere. The master alloy was re-melted twice to ensure compositional homogeneity. The melt was quenched by injecting on a copper spinning wheel in a melt spinner device. The resulting ribbons had a thickness of $30 \pm 3 \mu\text{m}$ and a width of $1.5 \pm 0.2 \text{ mm}$. The amorphous character of the alloy was checked by XRD showing no signature of crystalline phases. The relaxed samples were prepared annealing 30 min at 693 K while applying a static stress in order to avoid the generation of residual stresses when cooling again the sample. Differential scanning calorimetry (DSC) was performed using a NETZSCH 404 F3 equipment on both as-quenched and relaxed samples. The DSC curves (Fig. 1) show distinct shapes of the glass transition signal, with the expected overshooting in

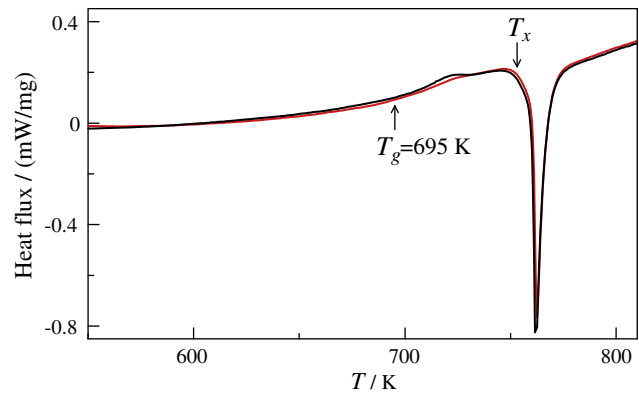


Fig. 1. DSC scans of the relaxed (black line) and as-quenched (red line) ribbons. The scans were performed at 10 K/min. (For interpretation of the references to colour in this figure legend, the reader is referred to the web version of this article.)

the relaxed glass [37], while the crystallization at higher temperatures is not affected by the pre-annealing protocol as the memory of the system is lost once heated above the glass transition.

The tensile DMA measurements were performed on melt spun ribbons applying a heating rate of 1 K/min and frequencies between 0.1 and 50 Hz. The frequency response was obtained by applying oscillating tensile strains of $1 \mu\text{m}$ amplitude on pieces of ribbon of about 10 mm length. Data was taken at temperature steps of 4 K from 500 K up to 750 K. The static stress-relaxation measurements were performed applying ‘instantaneous’ tensile deformations of amplitude $\varepsilon \sim 10^{-3}$, corresponding to an initial elastic stress of $\sigma_0 \sim 50\text{--}60 \text{ MPa}$, and then measuring the stress decay during 1 h. These measurements were performed in a Dynamomechanical-Analyzer Q800 of TA instruments.

The onset of glass transition is found at $T_g = 695 \text{ K}$ when measured by DSC at 10 K/min. Therefore, the annealing protocol is expected to drive the system to a sufficient relaxed state as to avoid significant structural changes below $\sim 690 \text{ K}$ while heating at 1 K/min, thus ensuring the mechanical response $E^*(\omega, T)$ corresponds to an isoconfigurational glassy state.

3. Results

Fig. 2 (top) shows the imaginary part of $E^*(\omega, T)$ of the relaxed ribbons as function of temperature for different frequencies. Fig. 2 (bottom) shows $E''(\omega, T)$ measured at constant $\omega = 2\pi \text{ s}^{-1}$ in as-quenched and relaxed samples, showing the reduction of the excess wing by annealing. Following the same method as in Ref. [38], the data sets obtained at each temperature were fitted to the CC-function of Eq. (3). The value of $E_0(T)$ is taken constant and equal to $E_0 = E'(T = 500 \text{ K})$ and the two fitting parameters are then $\alpha(T)$ and $\tau(T)$. The fitting CC-functions at some selected temperatures are shown in the inset of Fig. 2 (top). For the relaxed samples, the values of $\alpha(T)$ show some dispersion around an average value $\alpha = 0.35 \pm 0.06$ with no clear tendency to increase or decrease with temperature. The inset of Fig. 1 (bottom) shows the E'' data points collected for all temperatures and frequencies as a function of $\omega\tau(T)$. Within the frequency and temperature window explored, the data is well described by a single peak with no observable change in the slope of the high-frequency wing, which would be indicative of a merged secondary process [39].

The $\tau(T)$ values obtained by fitting Eq. (3) to the experimental data are depicted in Fig. 3. The glass transition, defined as $\tau(T_g) = 10^2 \text{ s}$, is found at $T_g = 692 \text{ K}$. The change from equilibrium to non-equilibrium dynamics is also clearly seen, the solid lines correspond to VFT and AGV functions with parameters $\tau_0 = 6 \times 10^{-13} \text{ s}$, $B = 6220$, $T_0 = 512 \text{ K}$ and $T_f = 694 \text{ K}$. The fragility parameter, calculated from the slope of the equilibrium curve at T_g , is found $m = 57$. The glass transition temperature and the fragility correspond well with the expected for $\text{Cu}_{46}\text{Zr}_{46}\text{Al}_8$ glass [40]. As seen in the inset of Fig. 2 (top), at temperatures well below T_g the DMA data covers only a small part of the high frequency tail of the

Download English Version:

<https://daneshyari.com/en/article/1608263>

Download Persian Version:

<https://daneshyari.com/article/1608263>

[Daneshyari.com](https://daneshyari.com)